Epilepsy Research 157 (2019) 106213

Contents lists available at ScienceDirect

Epilepsy Research

journal homepage: www.elsevier.com/locate/epilepsyres

Characterisation of medullary astrocytic populations in respiratory nuclei and alterations in sudden unexpected death in epilepsy

Smriti Patodia[a], Beatrice Paradiso[a,c], Matthew Ellis[b], Alyma Somani[a], Sanjay M. Sisodiya[a], Orrin Devinsky[d,1], Maria Thom[a,b,*,1]

[a] Departments of Clinical and Experimental Epilepsy, UCL Queen Square Institute of Neurology, London, WC1N 3BG, United Kingdom
[b] Departments of Neuropathology, UCL Queen Square Institute of Neurology, London, WC1N 3BG, United Kingdom
[c] Cardiovascular Pathology Unit, Department of Cardiac, Thoracic and Vascular Sciences, University of Padua Medical School, Padua, Italy
[d] New York University School of Medicine, Comprehensive Epilepsy Center, New York, United States

ARTICLE INFO

Keywords:
SUDEP
Astrocytes
ventrolateral medulla
Connexins
adenosine receptors

ABSTRACT

Central failure of respiration during a seizure is one possible mechanism for sudden unexpected death in epilepsy (SUDEP). Neuroimaging studies indicate volume loss in the medulla in SUDEP and a post mortem study has shown reduction in neuromodulatory neuropeptidergic and monoaminergic neurones in medullary respiratory nuclear groups. Specialised glial cells identified in the medulla are considered essential for normal respiratory regulation including astrocytes with pacemaker properties in the pre-Botzinger complex and populations of subpial and perivascular astrocytes, sensitive to increased pCO_2, that excite respiratory neurones. Our aim was to explore niches of medullary astrocytes in SUDEP cases compared to controls. In 48 brainstems from three groups, SUDEP (20), epilepsy controls (10) and non-epilepsy controls (18), sections through the medulla were labelled for GFAP, vimentin and functional markers, astrocytic gap junction protein connexin43 (Cx43) and adenosine A1 receptor (A1R). Regions including the ventro-lateral medulla (VLM; for the pre-Bötzinger complex), Median Raphe (MR) and lateral medullary subpial layer (MSPL) were quantified using image analysis for glial cell populations and compared between groups. Findings included morphologically and regionally distinct vimentin/Cx34-positive glial cells in the VLM and MR in close proximity to neurones. We noted a reduction of vimentin-positive glia in the VLM and MSPL and Cx43 glia in the MR in SUDEP cases compared to control groups ($p < 0.05–0.005$). In addition, we identified vimentin, Cx43 and A1R positive glial cells in the MSPL region which likely correspond to chemosensory glia identified experimentally. In conclusion, altered medullary glial cell populations could contribute to impaired respiratory regulatory capacity and vulnerability to SUDEP and warrant further investigation.

1. Introduction

Some cases of sudden and unexpected death in epilepsy (SUDEP) may result from a post-ictal central apnoea in which normal auto-resuscitative mechanisms fail (Ryvlin et al., 2013; Vilella et al., 2019). By definition post mortem examinations in SUDEP show no neuropathological cause of death. This criterion is likely to change as robust neuropathological associations are uncovered. We have recently identified cellular alterations in medullary respiratory regulatory nuclei (Patodia et al., 2018). Brainstem respiratory networks represent a complex interplay of multiple neuropeptides and modulating biogenic monoamines, that can adapt to repetitive physiological challenges (Smith et al., 2013), including intermittent hypercarbia following generalized seizures. Major brainstem respiratory groups include the pre-Bötzinger complex (preBötC) in the ventrolateral medulla (VLM), the serotonergic neurons of the medullary raphe (MR), the nucleus tractus solitarius (NTS) and retrotrapezoid nucleus (RTN); these regions have been more extensively studied in animals, but alterations in these networks could be relevant to SUDEP vulnerability.

Astrocytes can modulate neuronal activity via gliotransmission and dysfunction of astrocytes is implicated in epileptogenesis (Boison and Steinhauser, 2018; Pekny et al., 2016). Further, in experimental

Abbreviations: A1R, adenosine A1 receptor; Cx, connexin; MSPL, lateral medullary subpial layer; MR, Median Raphe; NTS, nucleus tractus solitarius; preBötC, pre-Bötzinger complex; RTN, retrotrapezoid nucleus; SUDEP, sudden unexpected death in epilepsy; VLM, ventrolateral medulla

* Corresponding author at: Department of Neuropathology, UCL Queen Square Institute of Neurology, Queen Square, London, WC1N 3BG, United Kingdom.
E-mail address: M.Thom@ucl.ac.uk (M. Thom).

[1] Joint last co-authorship.

https://doi.org/10.1016/j.eplepsyres.2019.106213
Received 5 July 2019; Received in revised form 20 September 2019; Accepted 30 September 2019
Available online 01 October 2019
0920-1211/

models, regulatory roles of brainstem glia in respiratory homeostasis have been demonstrated (Czeisler et al., 2019). Specialised superficial medullary glial are chemosensitive to pCO_2 levels and stimulate respiratory neurones via connexin channels and ATP (Huckstepp et al., 2010). Astrocytes in the VLM, functionally coupled to somatostatin-expressing pre-BötC neurones (Ikeda et al., 2017) are involved in adaptive respiratory responses during physiological challenges (Sheikhbahaei et al., 2018b). Altered medullary glial cell populations in sudden infant death (SIDS) (Hunt et al., 2016) an event with many parallels to SUDEP, are hypothesised to contribute to the mechanisms of death in these cases (Mitterauer, 2011). In addition, experimental data from several SUDEP models found post-ictal brainstem spreading depolarisation mediates the irreversible respiratory collapse (Aiba and Noebels, 2015; Loonen et al., 2019); although glial cells are physiologically relevant to cortical spreading depolarisation (Rovegno and Saez, 2018; Seidel et al., 2016) their contribution to brainstem spreading depolarisation (or indeed confirmation of spreading depolarisation in SUDEP) has yet to be demonstrated.

There is limited data regarding the distribution and morphology of human medullary astrocytes in relation to any specialised respiratory functions (Rusu et al., 2013; SheikhBahaei et al., 2018a). Our aim, in a series of adult post mortems in patients with epilepsy and SUDEP, was to further characterise the distribution and morphology of medullary astrocytes in respiratory nuclei.

2. Methods

2.1. Case selection

We studies medullas from 48 post mortem cases obtained from the Epilepsy Society Brain and Tissue Bank (ESBTB) at UCL, through Brain UK (pathology department at Derriford Hospital, Plymouth) and the MRC sudden death brain bank in Edinburgh. Tissue from all cases was retained with era-appropriate consent and the project has ethical approval (NRES17/SC/0573). The cases were acquired from post mortem examinations conducted between 1999 to 2017 and included 20 SUDEP cases, 10 Epilepsy controls (EPC; epilepsy with non-SUDEP cause of death) and 18 non-epilepsy controls (NEC). The SUDEP group included 11 definite SUDEP cases (complete and negative autopsy including toxicology), the remaining 9 being probable or possible SUDEP according to current definitions (Nashef et al., 2012). Our SUDEP and EPC groups included 7 cases with Dravet syndrome due to *SCN1A* mutations; no genotyping data was available on the remaining 23 epilepsy cases. The NEC group included 14 cases with sudden death (non-neurological, non-epilepsy sudden death). The clinical details of the groups, including mean age at death are summarised in Table 1.

2.2. Tissue preparation and quantitation methods

For all cases, a single 5 mm thick block was selected from the caudal medulla (axial level between obex 2–13 mm). Serial sections were cut through the block at 20 µm thickness using the Tissue-Tek AutoSection automated microtome (Sakura Finetek, U.S.A. Inc) and the obex level was determined on a cresyl violet stained section using a standard atlas (Paxinos and Huang, 1995). Immunostaining, including double labelling, for a glial marker panel was carried out (Table 2) using standard techniques (further detailed in additional methods file). Nestin and delta-GFAP showed suboptimal immunolabelling across cases and were therefore not included in further analysis.

Labelled astrocytic populations were quantified in defined regions of interest (ROI) in the medulla to include regions both with and without known respiratory regulatory control as detailed: **ROI1** the ventro-lateral medulla (VLM) to include the pre-Botzinger complex (pre-BötC) [Inspiratory nucleus (Bouras et al., 1987; Ikeda et al., 2017; Schwarzacher et al., 2011; Stornetta et al., 2003), **ROI2** the Median Raphe (MR) [Serotonergic neurones modulate respiratory nuclei, including pre-BötC, in conditions of hypercapnia (Benarroch, 2014) (Richerson, 2004)], **ROI3** the subventricular zone of IVth ventricle (SVZ) [non-respiratory regulatory region], **ROI4** the lateral medullary surface subpial layer (MSPL) [respiratory modulation shown experimentally as detailed above (Huckstepp et al., 2010)], **ROI5** the solitary tract (ST)/NTS region [chemosensory neurones project to VLM/ pre-BötC modulating respiration (Cui et al., 2016; Epelbaum et al., 1994; Smith et al., 2013; Spirovski et al., 2012), and **ROI6** the inferior olive nucleus [non-respiratory regulatory region]. The anatomical co-ordinates used to define these ROI in each case are as previously described ((Patodia et al., 2018); detailed in Fig. 1A). Slides were scanned with a Leica SCN400 F digital slide scanner (Leica Microsystems, Wetzlar, Germany) at 40x magnification. GFAP sections, due to the density of labelled processes and difficulty to distinguish individual cells, were analysed with Definiens Tissue Studio software 3.6 (Definiens AG, Munich, Germany); an intensity threshold was set for all cases and the total labelling index (LI) (percentage area stained by cells and processes) for each ROI was measured (Table 2). For Vimentin and Cx43, scanned slides were viewed on Leica Slidepath software at 20x magnification, the ROI annotated (as detailed in Fig. 1a), 5 random fields (area 0.5 mm^2) per ROI on each side captured and all immunopositive cells counted by manual tagging (expressed as cells/μm^2). For the MSPL, only regions of the medulla with an intact subpial layer and overlying meninges were evaluated. In cases with hemi-brain stem sections (Fig. 1b) only one side was evaluated; in other cases, both left and right sides were evaluated and the measurements averaged for ROIs. Double labelling co-localisation was evaluated qualitatively with confocal imaging using ZEISS LSM 880 laser scanning microscope with Airyscan and an Zeiss Axio Imager Z2 fluorescent microscope (Zeiss, Göttingen, Germany) in each ROI.

Table 1
Summary of cases included in study, clinical and post mortem data.

Group	Gender F : M	Mean age at PM (range)	Mean onset of epilepsy (Duration)	Mean obex. (range)	Mean PMI and FT (days)	Number of cases in each study
SUDEP N = 20	7 : 13	33 years (1 -59)	10.5 (19 years)	5.9 (2-13 mm)	2.9 (34 days)	GFAP (14) Vimentin (16) Cx43 (16) AD1R (6)
Epilepsy Controls N = 10	4 :6	57 years (5-84)	13.8 (26.9 years)	6 (3-10.5 mm)	2.1 (48 days)	GFAP (5) Vimentin (10) Cx43(10)
Controls N = 18	7 : 11	40.8 years (23-80)	N/A	6.2 (2.5-10 mm)	3.4 (15 days)	GFAP (12) Vimentin (11) Cx43 (10) AD1R (4)

AD1R = adenosine 1R receptor, Cx = connexin, FT = fixation times, PM = post mortem, PMI = post mortem interval, SUDEP = Sudden and unexpected death in epilepsy.

2.3. Statistical analysis and clinico-pathology correlations

Statistical analysis was carried out using SPSS version 22 (IBM corporation, CA, USA) using Mann-Whitney, Kruskall Wallis and Spearman's correlations for non-parametric data between the cause of death groups with p values of < 0.05 taken as significant. For graphical representation of data, Graphpad Prism 7 (University of California, San Diego) was used.

Table 2
Immunohistochemistry panel and regional quantitative methods. Detail of methods is included in supplemental file and for delineation of ROI refer to Fig. 1A (ROI1 the ventrolateral medulla, ROI2 the Median Raphe (MR), ROI 3 the subventricular zone of IVth ventricle, ROI4 the lateral medullary surface subpial layer, ROI5 the solitary tract, ROI6 the inferior olive nucleus.).

Immunohisto chemistry marker/stain	Company, clone and dilution	Quantitative method / Regions of interest (ROIs) evaluated	
GFAP	DAKO ZO334 (Polyclonal, Rabbit, 1: 2500)	Whole slide scanning image analysis	ROI 1, 5, 6
Vimentin	DAKO M0725 (Monclonal, Mouse, 1 : 2000)	Quantitative cell counts	RO1 : 1,2,3,4
Connexin 43	Thermofisher Scientific 13-8100 (Monoclonal, Mouse, 1 : 400)	Quantitative cell counts	RO1 : 1,2,3,4
Adenosine A1 Receptor	Abcam ab124780 (Monoclonal, Rabbit 1:200)	Qualitative evaluation	All ROI
GFAP/ Cx43	1:1500/1:2000	Qualitative Evaluation for co-localisation	All ROI
GFAP/Vimentin	1:1500/1:400	Qualitative Evaluation for co-localisation	All ROI
Vimentin/Cx43	1:2000/1:400	Qualitative Evaluation for co-localisation	All ROI
Vimentin/ Adenosine A1 Receptor	1:500/1:200	Qualitative Evaluation for co-localisation	All ROI

3. Results

3.1. GFAP

Dense labelling of glial cells and processes was present in all medullary regions (Fig. 1B) including a prominent horizontal subpial band of cells (Figs. 1E, 2 D). There was a qualitative impression of reduced density of GFAP-positive processes in the VLM in epilepsy cases compared to NEC (Fig. 1B–D, F–H). Quantitative evaluation showed lower mean labelling index in the VLM in epilepsy groups that was not statistically different from controls (Fig. 3A). There was also no significant difference in GFAP labelling between SUDEP, EPC and NEC for any other ROI or in relation to obex level, age of death, post mortem interval or fixation time.

3.2. Vimentin

Labelling of vascular channels throughout the medulla, as well as astrocytic cells in the area postrema, was noted. Within all ROI, less frequent and morphologically more diverse vimentin-positive astroglial cell types were seen compared to GFAP. A band of vimentin-positive cells was present beneath the lateral medulla subpial surface extending from the arcuate nuclei along the lateral medullary border (Fig. 2A), some with long processes running both parallel to the surface and extending toward the lateral medulla. In the VLM, single multipolar cells with complex branching processes were interspersed between neurones, some with large cell bodies and long processes, extending towards both neurones and capillaries (Fig. 2E). In the region of the ST/NTS, small multipolar vimentin-positive glia and processes were also observed. The MR midline region showed prominent large vimentin-positive cells with elongated processes running mainly bi-directionally along the raphe, particularly the dorsal raphe obscurus nucleus (Fig. 2I), extending processes around neurones and occasionally towards the lateral medulla. In the SVZ, a distinct row of subependymal vimentin-positive multipolar cells was present with elongated processes (Fig. 2O). Quantitative analysis in ROI showed lower densities of vimentin-positive cells in all regions in SUDEP compared to NEC ($p < 0.05$); in addition lower vimentin-positive cell densities in the VLM, SVZ and MSPL were observed in SUDEP compared to EPC group ($p < 0.05$ to $p < 0.005$) (Fig. 3B). There was no significant correlation between vimentin-positive cell densities and obex level, post mortem interval or fixation time over all cases or with age in the cause of death groups.

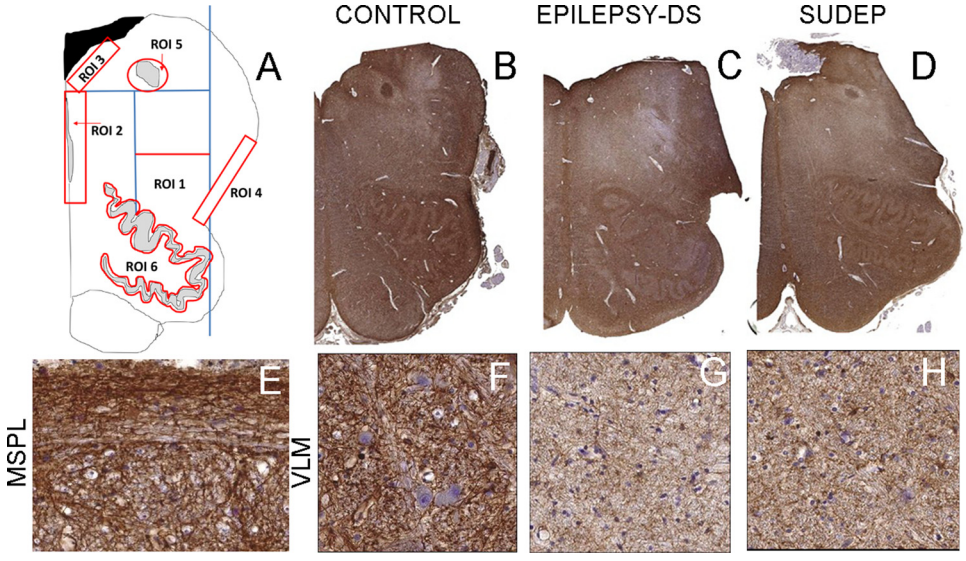

Fig. 1. Regions of interest and GFAP positive labelling in medulla.
A. Regions of interest included in the quantitative analysis. **ROI 1:** The ventrolateral medulla quadrant (VLM) was outlined geometrically on each section using co-ordinates from clearly defined anatomical landmarks of the medullary midline, the inferior olive nuclei and the central recess of the fourth ventricle as described previously (Patodia 2018). **ROI 2:** The Medullary Raphe (MR) ROI extended from the fourth ventricle to the olive ventrally and abutted the midline, this ensured inclusion of the regions with serotonergic neurones in both raphe obscurus and raphe pallidus. **ROI 3:** The sub ventricular zone (SVZ), the region immediately beneath the ependymal layer extending from the ventricle edge as inner border and from the midline to lateral margin. **ROI 4:** The lateral medullary subpial layer (MSPL), the surface of the medulla dorsal to the olive recess and overlying the lateral border of the VLM region using the subpial layer as the outer border. **ROI5:** The solitary tract region (ST) was identified in the dorsal medulla as centre of circular ROI to include nucleus of solitary tract but not extending to its ventricular border. **ROI6:** The nucleus of the inferior olive was outlined in its entirety following the contours of the nucleus. The dorsal and medial accessory olivary nuclei were not included in this ROI. **B.** GFAP stained sections of hemi-brainstem showing diffuse and intense labelling through an axial section of medulla in non-epilepsy control case. **C.** In epilepsy controls (case shown with confirmed Dravet syndrome (DS)) there was an impression of reduced GFAP compared to non-epilepsy controls in the region of the reticular formation and VLM and **D.** also in SUDEP cases. Regions from the VLM shown as rectangles in B, C, D are illustrated at higher magnifications in figures **F, G, H** respectively showing the variable dense meshworks of GFAP processes surrounding neurones. **E.** The lateral medullary subpial layer with GFAP process running in organised bundles in longitudinal orientation along the surface. Bar equivalent to 5 mm (B–D), 50 µm (E–H).

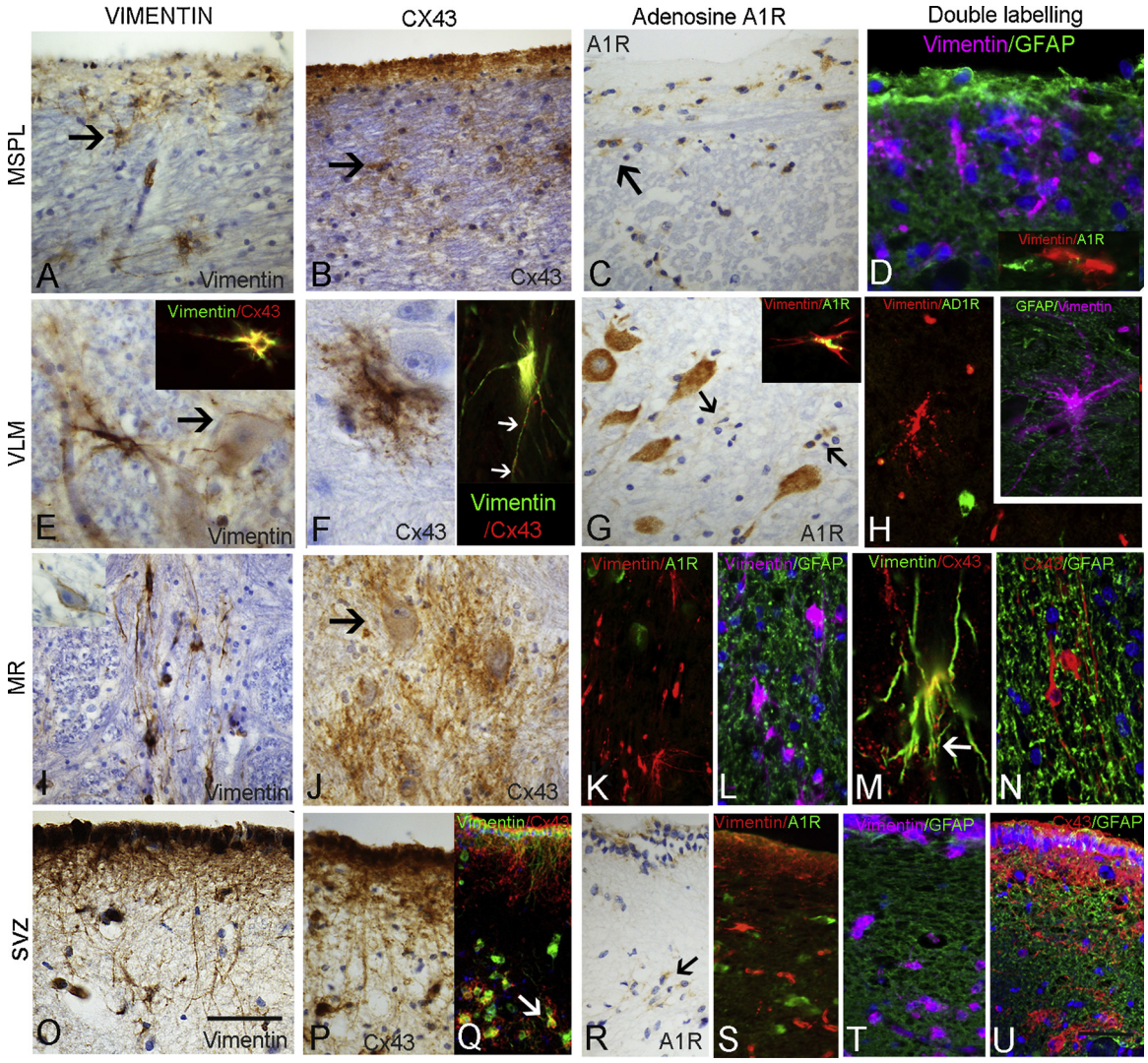

Fig. 2. Vimentin, Connexin 43 (Cx43) and Adenosine A1R receptor expression in regional medullary glial cells and double labelling with GFAP.
A. Medullary subpial layer (MSPL) with prominent numbers of single vimentin-positive multipolar glial cells (arrow), occasionally with long processes extending into lateral medulla. **B.** A similar pattern of labelling was observed with Cx43 with single cells showing bushy processes in the immediate subpial region of the lateral medulla (arrow). **C.** A1R also highlighted prominent single glial cells in the MSPL region (arrow) with cytoplasmic labelling. **D.** Double labelling for GFAP with vimentin and adenosine A1R with vimentin showed distinct cell populations with little co-localisation. **E. Ventrolateral medulla (VLM)** with prominent single medium to large vimentin-positive cells with exuberant processes; proximity and extension of cellular processes to local neurones (arrow) and to capillaries was noted. Insets in E and F show frequent co-localisation of labelling with vimentin and Cx43, with Cx43 often showing a characteristic punctate labelling along vimentin positive cell processes (arrows). **F.** Cx43 positive cells in the VLM were scattered and relatively infrequent but often with bushy and beaded processes and in proximity to neurones. **G.** Adenosine A1 receptor (A1R) showed intense cytoplasmic labelling of neurones in the VLM but scattered small glial cells were also present (arrows); inset shows rare co-localisation of labelling with vimentin and A1R. **H.** VLM highlighting mainly distinct cellular labelling of glial cells with vimentin and A1R and in inset with GFAP. **I. Medullary raphe (MR)** with prominent vimentin positive glial with elongated processes orientated along the axis of the nuclear group. *J.* Cx43 showed clusters of bushy glia with punctate labelling, some enveloping neurones (arrow). **K.** A1R did not co-localise with vimentin positive glia in the raphe and **L.** Vimentin positive glia were also distinct from GFAP labelled glial processes in this region. **M.** Cx43 and vimentin showed frequent cellular co-localisation and punctate Cx43 labelling along cell processes was a prominent feature (arrow). **N.** Cx43 and GFAP did not show distinct co-localisation in MR cell populations. **O. Subventricular zone (SVZ)** and vimentin with prominent labelling of elongated processes extending from the overlying ependymal layer and a band of single positive glial cells; **P.** A similar pattern of cell labelling was observed with Cx43 in SVZ and **Q.** showing frequent co-localisation of labelling in cells (arrow). **R.** AR1 highlighted single glial cells in the SVZ (arrow) but **S.** no co-localisation observed with vimentin. **T.** GFAP stain did not co-localise with vimentin positive glia in the SVZ or **U.** with Cx43. Scale Bar equivalent to 50 μm in A–D,G,I,J,0-U and 30 μm E–H and K–N.

3.3. Connexin 43

No neuronal labelling was observed. Scattered glial cells were labelled, with a regional distribution similar to vimentin. Cx43 labelling of the ependymal cells of the IVth ventricle, area postrema and occasional blood vessels, was present. A band of Cx43 labelling was noted in the MSPL (Fig. 2B), but was intermittent and variable between cases; scattered small Cx43-positive cells were also seen underlying this region (Fig. 2B). Infrequent, intensely labelled multipolar bushy Cx43-positive cells were noted in the NTS and VLM (Fig. 2F), some in close proximity to neurones. In the midline raphe, prominent punctate labelling forming bushy masses of Cx43-positive glial cells was seen, some enveloping neurones of the midline raphe (Fig. 2J). Intense Cx43 labelling was also seen in SVZ glial cells and occasional single Cx43-positive cells also noted in the XIIth cranial nerve nucleus and inferior olive. Quantitative analysis confirmed variability of labelling between cases, with overall significantly lower Cx43-positive cell densities in the MR in SUDEP than EPC group ($p < 0.05$); there were also lower Cx43-

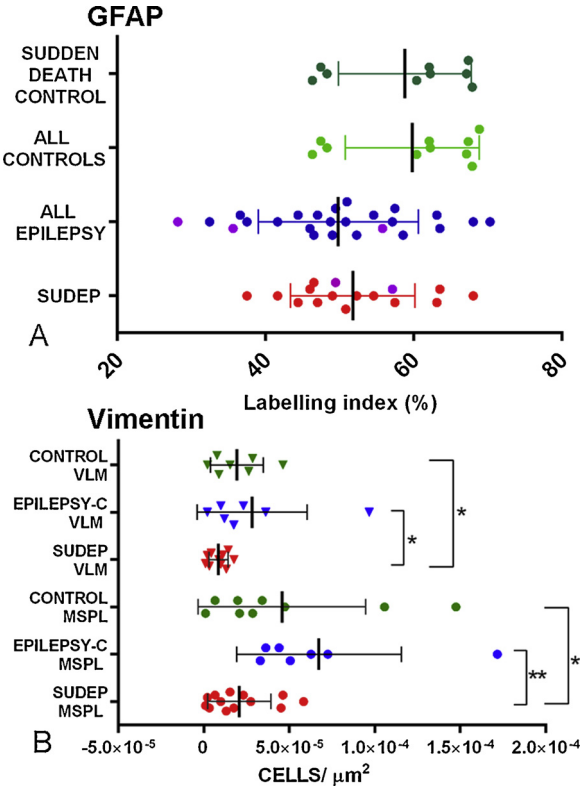

Fig. 3. Quantitative analysis.
A. Scatter graph of GFAP showing the ventrolateral medulla (VLM) region only; SUDEP and epilepsy group were lower but not significantly lower compared to non-epilepsy controls (one outlier on the graphs in the control group is not shown). The Dravet syndrome cases in the epilepsy control and SUDEP group are highlighted in purple but these cases were not statistically different from other SUDEP or epilepsy controls as a group. **B.** Scatter graph of vimentin quantitative analysis with significantly lower cell density in SUDEP group compared to epilepsy controls ($p = 0.045$) and non-epilepsy controls ($p = 0.02$) in the VLM. SUDEP cases also showed lower cell densities in the lateral medullary subpial layer (MSPL) compared to epilepsy controls ($p = 0.002$) and non-epilepsy control groups ($p = 0.026$).

positive cell densities in the MR in SUDEP compared to NEC cases with sudden death ($p < 0.05$). There was no significant difference in Cx43 labelling between SUDEP, EPC and NEC for other ROI or in relation to post mortem interval or fixation time. There was a positive correlation with Cx43 and obex level in the SVZ ROI only ($p < 0.05$). In the three cause of death groups there was a positive correlation with age of death and Cx43 cell density in the VLM ROI in SUDEP ($p < 0.05$) and in the MSPL in both SUDEP ($p < 0.005$) and EPC ($p < 0.05$) but not for any region in the NEC group.

There was positive correlation between quantitative measures for vimentin and Cx43 in MSPL, MR and SVZ ROI over all cases ($p < 0.01$ to 0.005), but no correlation for either marker with GFAP. There was no significant difference for any measure in Dravet syndrome cases compared to other SUDEP or EPC cases.

3.4. Adenosine A1 receptor (A1R)

There was intense cytoplasmic labelling for A1R in neuronal populations in the medulla including the VLM region (Fig. 2G). A1R labelling of glial populations was noted, particularly in the MSPL (Fig. 2C), VLM (Fig. 2G) and SVZ (Figure 2R) in both control and SUDEP cases. Cellular labelling was concentrated in the perikarya; elaborate cell processes were not observed with A1R. Due to the smaller number of cases studied this was not quantitatively evaluated.

3.5. Double labelling studies

GFAP with vimentin showed labelling of distinct glial cell populations in the MSPL ROI with little evidence of co-localisation (Fig. 2D), and also in the VLM (Fig. 2H inset), MR (Fig. 2L) and SVZ (Fig. 2T). There were similar findings for GFAP with Cx43 in these regions (shown for SVZ in Fig. 2U). In contrast, frequent cellular co-localisation of vimentin and Cx43 was observed in all regions including VLM (Fig. 2E, F insets), MR (Fig. 2M) and SVZ (Fig. 2Q), although in the VLM and MSPL not all vimentin positive cells were Cx43 positive. A distinctive finding was that of prominent Cx43 positive puncta on elongated vimentin-positive glial cell processes in the VLM (Fig. 2F, inset) and more prominently in the MR (Fig. 2M), including at branch points of cell processes. Rare AD1R/vimentin co-localisation in glial cells was noted in the VLM (Fig. 2G inset); in the MSPL (Fig. 2D inset) MR (Fig. 2K) and SVZ (Fig. 2S) however, AD1R and vimentin predominantly labelled intermingled but distinct populations of cells.

4. Discussion

We identified morphologically diverse astrocytic cell types in the human medulla, including distinctive vimentin, Cx43 and AD1R expressing cells in nuclei associated with respiratory regulation in the VLM and MR as well as on the medullary surface and, further to this, a relative deficit of some cell types in SUDEP compared to controls. Although no functional studies are feasible on post mortem samples, their specific morphology, immunophenotype, regional distribution, intimate association with local neurones and similarities to descriptions in animal models (SheikhBahaei et al., 2018a), suggests these are specialised glial cells with roles in respiratory modulation. These alterations in SUDEP cases could suggest brainstem glial dysfunction may contribute to pathophysiological mechanisms.

Sudden and unexpected death in epilepsy is the commonest cause of death in young patients with chronic and poorly controlled seizures (Devinsky et al., 2016). Several lines of evidence implicate brainstem medullary dysfunction. MRI studies in SUDEP found volume loss in autonomic brainstem regions including the medulla (Mueller et al., 2014, 2018) and recent functional imaging has addressed altered connectivity between cortical autonomic regulatory brain regions and the brainstem (Allen et al., 2019). In SIDS, which shares some similarities to SUDEP (including death in sleep in the prone position, male predominance and negative post mortem findings) impaired CO_2-driven arousal mechanisms are a potential pathogenic mechanism (Buchanan, 2019). Among other brainstem alterations identified in the more extensive post mortem studies conducted in SIDS (Machaalani and Waters, 2014), MALDI proteomics for GFAP intriguingly showed selective reductions in the ST and VLM regions compared to controls (Hunt et al., 2016). Neuropathology studies conducted in SUDEP are by comparison limited, but we recently observed alterations in neuropeptidergic and serotonergic neurones in the VLM in SUDEP (Patodia et al., 2018). In view of the emerging evidence of an astrogliopathy contributing to epileptogenesis (Pekny et al., 2016) as well as an hypothesised role in SIDS (Mitterauer, 2011) and the recognised physiological roles of medullary glia in respiratory regulation (Cohen et al., 2018), we speculated that medullary astrocytic populations may also be relevant in SUDEP.

We used the standard immunomarkers GFAP and vimentin to quantify the regional distribution of astroglial cells in the medulla. A single prior study reported specific niches of vimentin-positive glia in autonomic regulatory regions, including the raphe and solitary tract as well as cells forming a superficial layer of medullary astrocytes (Rusu et al., 2013). A rodent study confirmed the unique structural complexity of Pre-BötC astrocytes, with branching terminals, long processes and non-overlapping domains (SheikhBahaei et al., 2018a). Post-mortem fixed tissues cannot be used to assess cellular functional properties based on morphology; however, regional restricted

expression of Cx43 and A1R supports regionally specific metabolic functions and for gliotransmission. In the VLM, we noted vimentin-positive glia with long processes extending to both capillaries and neurones with punctate Cx43 expression that suggest local glial-neuronal networks. Astrocytes in the pre-BötC have pacemaker-like properties, periodic pre-inspiratory activation (Okada et al., 2012) and functional neuronal coupling (Oku et al., 2016). Astrocytic ATP release during hypoxia increases activity in the pre-BötC (Rajani et al., 2018), whereas blockade of gliotransmission in pre-BötC astrocytes impairs respiratory responses to hypoxia and hypercapnia (Sheikhbahaei et al., 2018b). Loss of VLM astrocytes in a Parkinson's disease model was associated with respiratory dysfunction (Fernandes-Junior et al., 2018). Our observation of significantly reduced VLM vimentin-positive cells in SUDEP cases could implicate dysfunctional glial-neuronal coupling and impaired inspiratory responses. Further, we identified a prominent population of elongated glial cells in the raphe with exuberant Cx43-positive processes associated with neurones, a significant reduction of this cell type in the SUDEP group and a correlation with age of patient in the epilepsy groups which could implicate chronic seizure modulation. Notably, SUDEP risk increases with epilepsy duration (Devinsky et al., 2016). Also, dysfunction of serotonergic systems is implicated in SUDEP (Murugesan et al., 2018; Richerson, 2013) and in experimental models, decreased responses of serotonergic neurons of medullary raphe has been shown following seizures (Zhan et al., 2016). We previously found a reduction in tryptophan hydroxylase-expressing neurones in the raphe in SUDEP (Patodia et al., 2018) ; as specialised glia have the functional capacity to amplify intrinsic chemosensitive neuronal responses through gliotransmitters (Eugenin Leon et al., 2016), a paucity in raphe glia could further impair these responses during seizures.

Experimental studies have also identified CO_2/H^+-sensitive astrocytes on the ventral medullary surface that activate respiratory circuits via connexin (Cx26) hemichannels (Huckstepp et al., 2010; Sobrinho et al., 2017), negatively modulated by extracellular adenosine through A1-receptors (Falquetto et al., 2018), stimulating brainstem respiratory neurones including in the MR and RTN. We report the novel finding of subsets of Cx43-positive and adenosine A1R-positive glia on the human medullary surface. We also observed a positive correlation in the density of Cx43 cells with age in epilepsy cases but not in controls, suggesting that cumulative seizure-effects could augment these cell types. The RTN has been putatively located in the human brainstem ventral to the facial nucleus and lateral to the superior olivary nucleus in the ponto-medullary junction (Rudzinski and Kapur, 2010). This region was not available in our medulla samples, nevertheless as structural abnormalities of PHOX-2B-expressing neurones populations in RTN have been described in SIDS (Lavezzi et al., 2012), study of this nucleus is warranted in SUDEP.

There is evidence for spreading depolarisation extending through the brainstem and solitary tract region during the terminal post-ictal event culminating in irreversible and fatal respiratory collapse in some SUDEP models (Aiba and Noebels, 2015; Loonen et al., 2019; Noebels, 2019). Astrocytes, through adenosine signalling (Seidel et al., 2016) or gap junctions (Rovegno and Saez, 2018) can initiate cortical spreading depolarisation. Brainstem spreading depolarisation has not been recorded in human SUDEP. Nevertheless our observation of altered specific medullary astrocytic populations, including in the periventricular location in proximity to the ST and NST, could be relevant to waves of post-ictal spreading depolarisation, which requires further study.

Limitations of post mortem studies include post mortem delays and different fixation times, which can influence quantitative immunohistochemistry. In addition, the procedure of brain removal can disrupt the delicate subpial surface astrocytes. We did not identify any correlation between pathology measures and post mortem intervals and fixation time and we were careful to carry out analysis only on regions with an intact subpial layer. The obex level of the medulla varied between cases; however, there were no significant differences between the groups. We did not have genetic analysis on all epilepsy and SUDEP cases; seven cases were genetically proven as Dravet syndrome with *SCN1A* mutations, but no differences in glial populations in this group from other SUDEP and EPC cases was observed, albeit the number of Dravet cases is small (Fig. 3A).

5. Conclusions

In summary, morphologically and regionally distinct vimentin, Cx43 and AD1R-positive glial cells are present in the human medulla and in known respiratory regulatory regions. We identified differences between SUDEP and control groups, including reduction of vimentin-positive glia in the VLM and MSPL and Cx43 glia in the MR, that may progress over the course of epilepsy and may be relevant to the impaired autonomic respiratory responses following seizures that contribute to SUDEP pathophysiology.

Declaration of Competing Interest

This study has ethical approval with appropriate consent for research for all cases included in the study. All data generated or analysed during this study are included in this published article. The authors have no conflicts of interest to declare.

Acknowledgments

UCL is part of the Center for SUDEP Research (CSR) and supported through the National Institute of Neurological Disorders And Stroke of the National Institutes of Health (Award Numbers neuropathology of SUDEP: 5U01NS090415 and SUDEP admin core grant: U01-NS090405). Epilepsy Society supports SMS, and through the Katy Baggott Foundation, supports the UCL Epilepsy Society Brain and Tissue Bank. This work was undertaken at UCLH/UCL who received a proportion of funding from the Department of Health's NIHR Biomedical Research Centres funding scheme. We are very grateful for provision of additional SUDEP and control material for this study from the following resources: The MRC Sudden Death Brain Bank in Edinburgh (cases detailed in additional methods file). Tissue samples were also obtained from David Hilton at Derriford Hospital as part of the UK Brain Archive Information Network (BRAIN UK) which is funded by the Medical Research Council and Brain Tumour Research.

Appendix A. Supplementary data

Supplementary material related to this article can be found, in the online version, at doi:https://doi.org/10.1016/j.eplepsyres.2019.106213.

References

Aiba, I., Noebels, J.L., 2015. Spreading depolarization in the brainstem mediates sudden cardiorespiratory arrest in mouse SUDEP models. Sci. Transl. Med. 7, 282ra246.
Allen, L.A., Harper, R.M., Lhatoo, S., Lemieux, L., Diehl, B., 2019. Neuroimaging of sudden unexpected death in epilepsy (SUDEP): insights from structural and resting-state functional MRI studies. Front. Neurol. 10, 185.
Benarroch, E.E., 2014. Medullary serotonergic system: organization, effects, and clinical correlations. Neurology 83, 1104–1111.
Boison, D., Steinhauser, C., 2018. Epilepsy and astrocyte energy metabolism. Glia 66, 1235–1243.
Bouras, C., Magistretti, P.J., Morrison, J.H., Constantinidis, J., 1987. An immunohistochemical study of pro-somatostatin-derived peptides in the human brain. Neuroscience 22, 781–800.
Buchanan, G.F., 2019. Impaired CO2-induced arousal in SIDS and SUDEP. Trends Neurosci. 42, 242–250.
Cohen, E.M., Farnham, M.M.J., Kakall, Z., Kim, S.J., Nedoboy, P.E., Pilowsky, P.M., 2018. Glia and central cardiorespiratory pathology. Auton. Neurosci.: Basic Clin. 214, 24–34.
Cui, Y., Kam, K., Sherman, D., Janczewski, W.A., Zheng, Y., Feldman, J.L., 2016. Defining preBotzinger complex rhythm- and pattern-generating neural microcircuits in vivo. Neuron 91, 602–614.

Czeisler, C.M., Silva, T.M., Fair, S.R., Liu, J., Tupal, S., Kaya, B., Cowgill, A., Mahajan, S., Silva, P.E., Wang, Y., Blissett, A.R., Goksel, M., Borniger, J.C., Zhang, N., Fernandes-Junior, S.A., Catacutan, F., Alves, M.J., Nelson, R.J., Sundaresean, V., Rekling, J., Takakura, A.C., Moreira, T.S., Otero, J.J., 2019. The role of PHOX2B-derived astrocytes in chemosensory control of breathing and sleep homeostasis. J. Physiol. 597, 2225–2251.

Devinsky, O., Hesdorffer, D.C., Thurman, D.J., Lhatoo, S., Richerson, G., 2016. Sudden unexpected death in epilepsy: epidemiology, mechanisms, and prevention. Lancet Neurol. 15, 1075–1088.

Epelbaum, J., Dournaud, P., Fodor, M., Viollet, C., 1994. The neurobiology of somatostatin. Crit. Rev. Neurobiol. 8, 25–44.

Eugenin Leon, J., Olivares, M.J., Beltran-Castillo, S., 2016. Role of astrocytes in central respiratory chemoreception. Adv. Exp. Med. Biol. 949, 109–145.

Falquetto, B., Oliveira, L.M., Takakura, A.C., Mulkey, D.K., Moreira, T.S., 2018. Inhibition of the hypercapnic ventilatory response by adenosine in the retrotrapezoid nucleus in awake rats. Neuropharmacology 138, 47–56.

Fernandes-Junior, S.A., Carvalho, K.S., Moreira, T.S., Takakura, A.C., 2018. Correlation between neuroanatomical and functional respiratory changes observed in an experimental model of Parkinson's disease. Exp. Physiol. 103 (10), 1377–1389.

Huckstepp, R.T., id Bihi, R., Eason, R., Spyer, K.M., Dicke, N., Willecke, K., Marina, N., Gourine, A.V., Dale, N., 2010. Connexin hemichannel-mediated CO2-dependent release of ATP in the medulla oblongata contributes to central respiratory chemosensitivity. J. Physiol. 588, 3901–3920.

Hunt, N.J., Phillips, L., Waters, K.A., Machaalani, R., 2016. Proteomic MALDI-TOF/TOF-IMS examination of peptide expression in the formalin fixed brainstem and changes in sudden infant death syndrome infants. J. Proteom. 138, 48–60.

Ikeda, K., Kawakami, K., Onimaru, H., Okada, Y., Yokota, S., Koshiya, N., Oku, Y., Iizuka, M., Koizumi, H., 2017. The respiratory control mechanisms in the brainstem and spinal cord: integrative views of the neuroanatomy and neurophysiology. J. Physiol. Sci.: JPS 67, 45–62.

Lavezzi, A.M., Weese-Mayer, D.E., Yu, M.Y., Jennings, L.J., Corna, M.F., Casale, V., Oneda, R., Matturri, L., 2012. Developmental alterations of the respiratory human retrotrapezoid nucleus in sudden unexplained fetal and infant death. Auton. Neurosci.: Basic Clin. 170, 12–19.

Loonen, I.C.M., Jansen, N.A., Cain, S.M., Schenke, M., Voskuyl, R.A., Yung, A.C., Bohnet, B., Kozlowski, P., Thijs, R.D., Ferrari, M.D., Snutch, T.P., van den Maagdenberg, A., Tolner, E.A., 2019. Brainstem spreading depolarization and cortical dynamics during fatal seizures in Cacna1a S218L mice. Brain 142, 412–425.

Machaalani, R., Waters, K.A., 2014. Neurochemical abnormalities in the brainstem of the Sudden Infant Death Syndrome (SIDS). Paediatr. Respir. Rev. 15, 293–300.

Mitterauer, B.J., 2011. The gliocentric hypothesis of the pathophysiology of the sudden infant death syndrome (SIDS). Med. Hypotheses 76, 482–485.

Mueller, S.G., Bateman, L.M., Laxer, K.D., 2014. Evidence for brainstem network disruption in temporal lobe epilepsy and sudden unexplained death in epilepsy. Neuroimage Clin. 5, 208–216.

Mueller, S.G., Nei, M., Bateman, L.M., Knowlton, R., Laxer, K.D., Friedman, D., Devinsky, O., Goldman, A.M., 2018. Brainstem network disruption: a pathway to sudden unexplained death in epilepsy? Hum. Brain Mapp. 39 (12), 4820–4830.

Murugesan, A., Rani, M.R.S., Hampson, J., Zonjy, B., Lacuey, N., Faingold, C.L., Friedman, D., Devinsky, O., Sainju, R.K., Schuele, S., Diehl, B., Nei, M., Harper, R.M., Bateman, L.M., Richerson, G., Lhatoo, S.D., 2018. Serum serotonin levels in patients with epileptic seizures. Epilepsia 59, e91–e97.

Nashef, L., So, E.L., Ryvlin, P., Tomson, T., 2012. Unifying the definitions of sudden unexpected death in epilepsy. Epilepsia 53, 227–233.

Noebels, J.L., 2019. Brainstem spreading depolarization: rapid descent into the shadow of SUDEP. Brain 142, 231–233.

Okada, Y., Sasaki, T., Oku, Y., Takahashi, N., Seki, M., Ujita, S., Tanaka, K.F., Matsuki, N., Ikegaya, Y., 2012. Preinspiratory calcium rise in putative pre-Botzinger complex astrocytes. J. Physiol. 590, 4933–4944.

Oku, Y., Fresemann, J., Miwakeichi, F., Hulsmann, S., 2016. Respiratory calcium fluctuations in low-frequency oscillating astrocytes in the pre-Botzinger complex. Respir. Physiol. Neurobiol. 226, 11–17.

Paxinos, G., Huang, X.F., 1995. Atlas of the Human Brainstem. Academic Press, San Diego.

Patodia, S., Somani, A., O'Hare, M., Venkateswaran, R., Liu, J., Michalak, Z., Ellis, M., Scheffer, I.E., Diehl, B., Sisodiya, S.M., Thom, M., 2018. The ventrolateral medulla and medullary raphe in sudden unexpected death in epilepsy. Brain 141, 1719–1733.

Pekny, M., Pekna, M., Messing, A., Steinhauser, C., Lee, J.M., Parpura, V., Hol, E.M., Sofroniew, M.V., Verkhratsky, A., 2016. Astrocytes: a central element in neurological diseases. Acta Neuropathol. 131, 323–345.

Rajani, V., Zhang, Y., Jalubula, V., Rancic, V., SheikhBahaei, S., Zwicker, J.D., Pagliardini, S., Dickson, C.T., Ballanyi, K., Kasparov, S., Gourine, A.V., Funk, G.D., 2018. Release of ATP by pre-Botzinger complex astrocytes contributes to the hypoxic ventilatory response via a Ca(2+) -dependent P2Y1 receptor mechanism. J. Physiol. 596, 3245–3269.

Richerson, G.B., 2004. Serotonergic neurons as carbon dioxide sensors that maintain pH homeostasis. Nat. Rev. Neurosci. 5, 449–461.

Richerson, G.B., 2013. Serotonin: the Anti-SuddenDeathAmine? Epilepsy Curr. Am. Epilepsy Soc. 13, 241–244.

Rovegno, M., Saez, J.C., 2018. Role of astrocyte connexin hemichannels in cortical spreading depression. Biochim. Biophys. Acta Biomembr. 1860, 216–223.

Rudzinski, E., Kapur, R.P., 2010. PHOX2B immunolocalization of the candidate human retrotrapezoid nucleus. Pediatr. Dev. Pathol. 13, 291–299.

Rusu, M.C., Dermengiu, D., Loreto, C., Motoc, A.G., Pop, E., 2013. Astrocitary niches in human adult medulla oblongata. Acta Histochem. 115, 296–300.

Ryvlin, P., Nashef, L., Lhatoo, S.D., Bateman, L.M., Bird, J., Bleasel, A., Boon, P., Crespel, A., Dworetzky, B.A., Hogenhaven, H., Lerche, H., Maillard, L., Malter, M.P., Marchal, C., Murthy, J.M., Nitsche, M., Pataraia, E., Rabben, T., Rheims, S., Sadzot, B., Schulze-Bonhage, A., Seyal, M., So, E.L., Spitz, M., Szucs, A., Tan, M., Tao, J.X., Tomson, T., 2013. Incidence and mechanisms of cardiorespiratory arrests in epilepsy monitoring units (MORTEMUS): a retrospective study. Lancet Neurol. 12, 966–977.

Schwarzacher, S.W., Rub, U., Deller, T., 2011. Neuroanatomical characteristics of the human pre-Botzinger complex and its involvement in neurodegenerative brainstem diseases. Brain 134, 24–35.

Seidel, J.L., Escartin, C., Ayata, C., Bonvento, G., Shuttleworth, C.W., 2016. Multifaceted roles for astrocytes in spreading depolarization: a target for limiting spreading depolarization in acute brain injury? Glia 64, 5–20.

SheikhBahaei, S., Morris, B., Collina, J., Anjum, S., Znati, S., Gamarra, J., Zhang, R., Gourine, A.V., Smith, J.C., 2018a. Morphometric analysis of astrocytes in brainstem respiratory regions. J. Comp. Neurol. 526, 2032–2047.

Sheikhbahaei, S., Turovsky, E.A., Hosford, P.S., Hadjihambi, A., Theparambil, S.M., Liu, B., Marina, N., Teschemacher, A.G., Kasparov, S., Smith, J.C., Gourine, A.V., 2018b. Astrocytes modulate brainstem respiratory rhythm-generating circuits and determine exercise capacity. Nat. Commun. 9, 370.

Smith, J.C., Abdala, A.P., Borgmann, A., Rybak, I.A., Paton, J.F., 2013. Brainstem respiratory networks: building blocks and microcircuits. Trends Neurosci. 36, 152–162.

Sobrinho, C.R., Goncalves, C.M., Takakura, A.C., Mulkey, D.K., Moreira, T.S., 2017. Fluorocitrate-mediated depolarization of astrocytes in the retrotrapezoid nucleus stimulates breathing. J. Neurophysiol. 118, 1690–1697.

Spirovski, D., Li, Q., Pilowsky, P.M., 2012. Brainstem galanin-synthesizing neurons are differentially activated by chemoreceptor stimuli and represent a subpopulation of respiratory neurons. J. Comp. Neurol. 520, 154–173.

Stornetta, R.L., Rosin, D.L., Wang, H., Sevigny, C.P., Weston, M.C., Guyenet, P.G., 2003. A group of glutamatergic interneurons expressing high levels of both neurokinin-1 receptors and somatostatin identifies the region of the pre-Botzinger complex. J. Comp. Neurol. 455, 499–512.

Vilella, L., Lacuey, N., Hampson, J.P., Rani, M.R.S., Sainju, R.K., Friedman, D., Nei, M., Strohl, K., Scott, C., Gehlbach, B.K., Zonjy, B., Hupp, N.J., Zaremba, A., Shafiabadi, N., Zhao, X., Reick-Mitrisin, V., Schuele, S., Ogren, J., Harper, R.M., Diehl, B., Bateman, L., Devinsky, O., Richerson, G.B., Ryvlin, P., Lhatoo, S.D., 2019. Postconvulsive central apnea as a biomarker for sudden unexpected death in epilepsy (SUDEP). Neurology 92 (3), e171–e182.

Zhan, Q., Buchanan, G.F., Motelow, J.E., Andrews, J., Vitkovskiy, P., Chen, W.C., Serout, F., Gummadavelli, A., Kundishora, A., Furman, M., Li, W., Bo, X., Richerson, G.B., Blumenfeld, H., 2016. Impaired serotonergic brainstem function during and after seizures. J. Neurosci. 36, 2711–2722.